A GAS IONIZATION SAMPLING ELECTROMAGNETIC SHOWER DETECTOR

TM-1010
2529.000
November 1980

M. Atac, D. Hanssen, H. Jensen, A. Tollestrup, and J. Urish
Fermi National Accelerator Laboratory, Batavia, IL 60510*

R. G. Kennett and R. Walker
California Institute of Technology, Pasadena, CA 91125

L. Nodulman
Argonne National Laboratory, Argonne, IL 60439

Abstract

The results of the tests of a prototype ionization sampling calorimeter are presented. Using proportional chambers interleaved with lead and sampling every 0.68 radiation length, we found an energy resolution of $24\%/\sqrt{E}$. Measurements of position resolution, lateral shower development, and hadron rejection are discussed.

Introduction

The tests of a proportional wire chamber calorimeter were undertaken as part of the prototyping work for the Colliding Beam Detector project at Fermilab. Ease of construction, spatial resolution, and the ease with which towers may be constructed from cathode pads make this an attractive system for our end cap calorimetry. Previous work[1,2] has shown the practicality of this technique in the construction of 4π detectors.

Calorimeter Construction

The calorimeter was built from 34 proportional wire chambers interleaved with lead plates. The chambers, see Fig. 1, had a 12 mm gap with 50 micron gold plated tungsten sense wires placed every 6 mm. The cells were separated by 100 micron copper-beryllium field wires at ground potential. Cathode strips run orthogonally to the wires on one side of the chambers. They were 6 mm center to center with a 1 mm gap between strips. The chambers were filled with a 50%-50% mixture of argon and ethane for all studies.

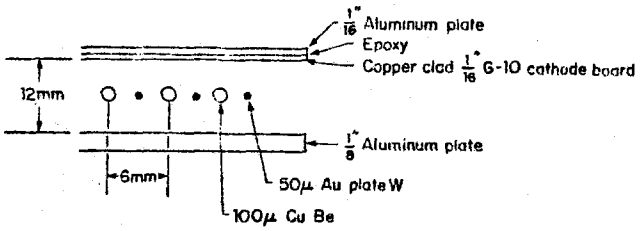

Fig. 1. Chamber construction.

All chambers were tested prior to use. Gain measurements along wires and from wire to wire within a given chamber showed an r.m.s. variation of less than 2.5% over an active area greater than 20 x 20 cm^2. Overall chamber gain was measured by averaging the response of the central wires in each chamber. On the basis of those measurements we were able to segregate the chambers into two groups of 8 and one group of 18 with a total gain variation within each group of not greater than 6%. When the calorimeter was assembled, we alternated "high gain" and "low gain" chambers within each group.

Measurements of gas gain as a function of several parameters resulted in the empirical relationship:

$$\frac{\Delta G}{G} = 15.8\,\frac{\Delta E}{E} - 15\,\frac{\Delta P}{P} + 6.3\,\frac{\Delta T}{T} - 1.3\,\frac{\Delta t}{t}$$

Where G is gas gain, E is high voltage, P is gas pressure, T is temperature, and t is gap thickness. Normal running voltage was 1450 volts, resulting in a gas gain of about 780.

The assembled calorimeter, see Fig. 2, had three independently read out sections. The first two sections were sampled every .68 radiation length, while the third section was sampled every 1.19 radiation length. Three high voltage supplies were used, one for each section.

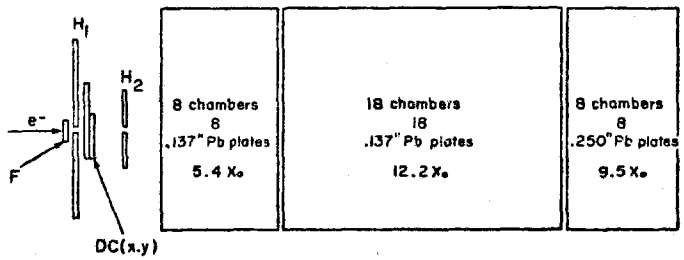

Fig. 2. Calorimeter segmentation showing beam counters and drift chambers. Each chamber represented 0.054 radiation length (3/16 in. aluminum).

The chambers were connected to a common intake gas manifold through individual flowmeters. All chambers were carefully leak checked, and their outputs connected to a common exhaust manifold. After a period of initial flushing, the flow rate was reduced to 10 cc/min. for each chamber. No adverse effects of this low flow rate were noted.

Readout Electronics

The wires and strips were grouped two-by-two in each chamber and daisy-chained to all corresponding wires or strips in a given section along the beam direction. This gave an effective cell width of 1.2 cm for both wires and strips.

Fig. 3 shows the electronics connection to the chambers. The 0.1 μF capacitor at the integrater input prevented any possible high voltage leakage through the 200 pF blocking capacitor and surface leakage around the cable ends from affecting the wire amplifiers. The 50 ohm resistor damped oscillations on the coaxial cable and improved the system noise.

The integrator, sample and hold, and differential amplifier were part of a single multiplexed ADC system.[3] Before a trigger, both the "before" and "after" switches are closed. The trigger causes the "before" switch to open, capturing the zero level of the integrator output. The integrator response to an input charge propogates down the delay line and is placed on the "after" sample and hold capacitor. The "after" sample and hold switch is then opened and the differential amplifier takes the appropriate difference between the "before" and "after" levels so as to provide a positive output to the ADC.

Because of limitations in the number of available channels, section 1 had 16 x 16 instrumented wire and strip pairs, or an instrumented area of about 19 x 19 cm^2. Sections 2 and 3 had 23 x 23 channels, or an area

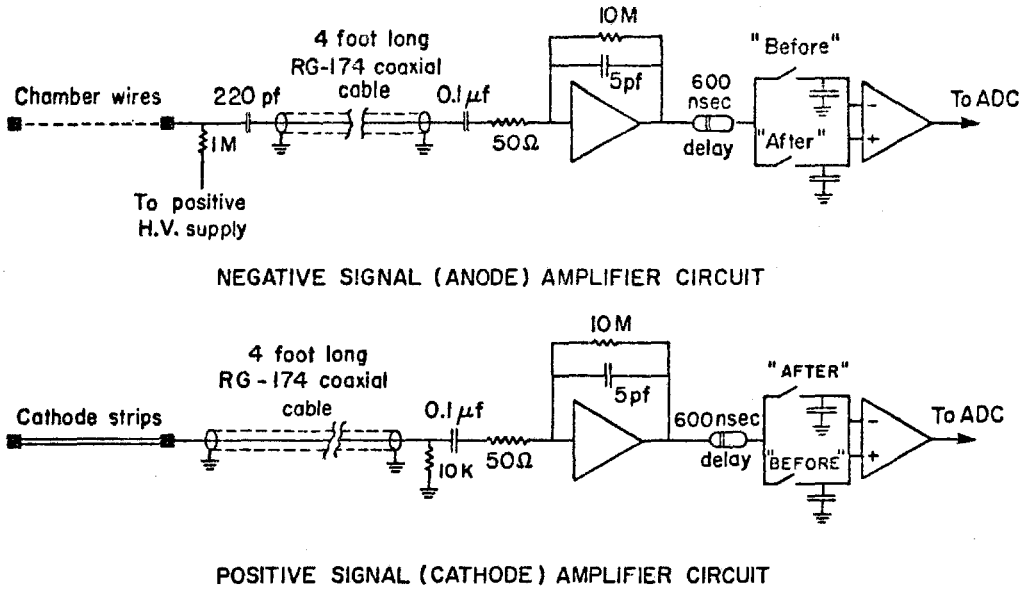

Fig. 3. Readout electronics.

of 27.6 x 27.6 cm^2. Incident particles were usually kept near the center of the instrumented area to minimize energy leakage out of the wings.

The data were collected and written on magnetic tape for offline analysis. Online analysis and diagnostics were implemented using the MULTI software package distributed by the Fermilab Computing Department.[4]

Calibration

Gas gain was monitored in one chamber of each section using the 22 KeV line of a Cd^{109} source with special high gain amplifiers. A typical source peak is shown in Fig. 4. It was possible to determine the source peak position to within 1%. Source triggers were admitted during the accelerator's interspill period so that we could monitor gas gain changes during a data run.

Electronics gain was initially measured using a charge injector at the amplifier inputs. The amplifiers were then connected to the chambers, and the field wires pulsed. This provided an easy way to see time dependent gain variations, and at the same time verify the integrity of the chamber to amplifier connections. We found the amplifiers to have an r.m.s. gain variation of 3%. Gain changes with time were insignificant.

Beamline and Trigger

The calorimeter was installed in the M5 beamline at Fermilab. The beam consisted primarily of pions with about 2% electrons at 40 GeV. Particle identification and beam trigger were provided by a series of Cherenkov detectors and scintillator counters. See Fig. 5.

An electron signal was obtained from the combination:

$$C1 \cdot C2 \cdot U \cdot D \cdot F \cdot \overline{H1} \cdot \overline{H2}$$

A pion signal was obtained from:

$$\overline{C1} \cdot \overline{C2} \cdot U \cdot D \cdot F \cdot \overline{H1} \cdot \overline{H2}$$

In addition, an upper level discriminator on F measured dE/dx and was used to veto multiple particles that did not diverge sufficiently to hit hole counter H1 or H2.

A pile-up gate was implemented that prevented a particle from generating a trigger when preceeded by another particle within 1 microsecond. A flag was set in a CAMAC register allowing offline rejection of events when a triggering particle was followed by another particle within the sensitive period of the readout system (1 microsecond).

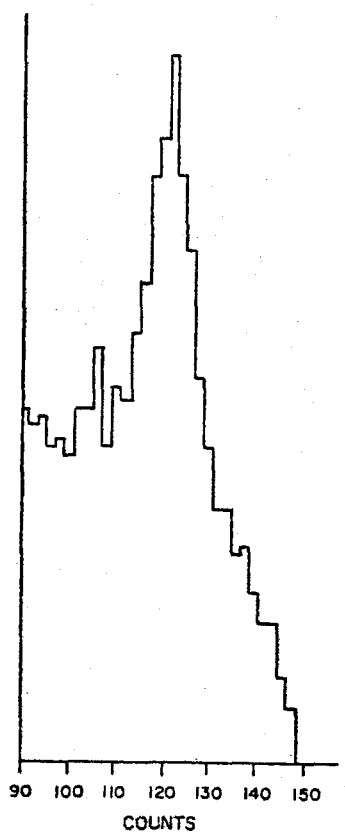

Fig. 4. Cd^{109} 22 KeV line used for gas gain measurement. Chamber was operated at 1450 volts.

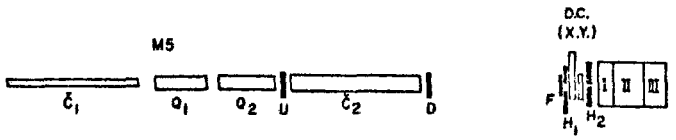

Fig. 5. M5 downstream layout. Cherenkov counters C1 and C2 tagged electrons. Scintillator counters U (up), D (down), and F (finger) indicated passage of a particle. Hole counters H1 and H2 determined the trigger beam size and indicated the presence of multiple particles from upstream secondary production. Drift chambers D. C. X and D. C. Y monitored particle position.

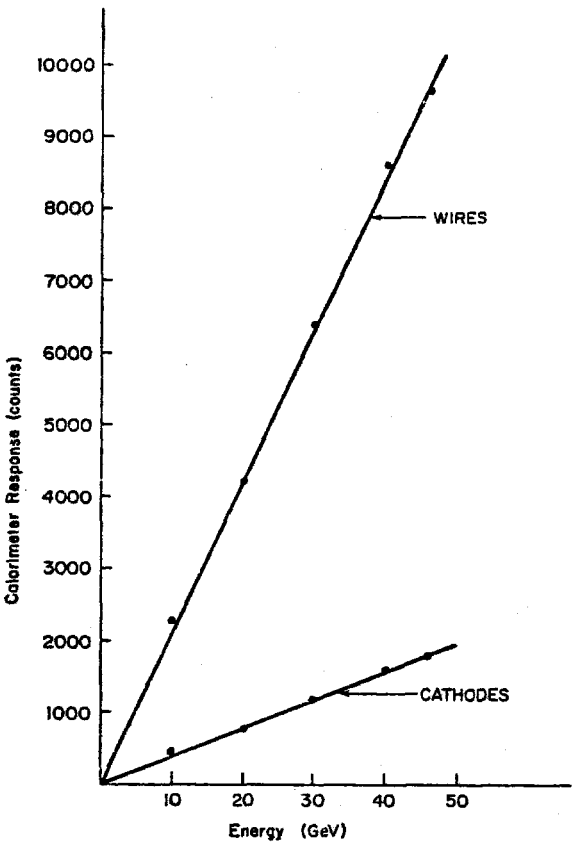

Fig. 6. Calorimeter response versus electron energy. Wire slope is 213 counts per GeV, strip slope is 39 counts per GeV.

Test Results

Fig. 6 shows the response of the calorimeter to different energy electrons. The wire response is seen to be 5.46 times the strip response. This is due to both cell geometry, which accounts for a factor of 4, and different gain of the charge amplifiers as a function of input capacitive loading.

Energy resolution for the wires is shown in Fig. 7, and shows a $24\%/\sqrt{E}$ dependence. Resolution is plotted both with the third section and without. The improvement seen when not using the third section shows that the noise contribution from that section is more significant than the signal content.

Cathode resolution is worse than wire resolution. about $27\%/\sqrt{E}$. This degradation is not well understood. It may be due to an unfavorable signal to noise ratio.

Fig. 8 shows a 40 GeV electron peak with the Gaussian fit used to determine the resolution.

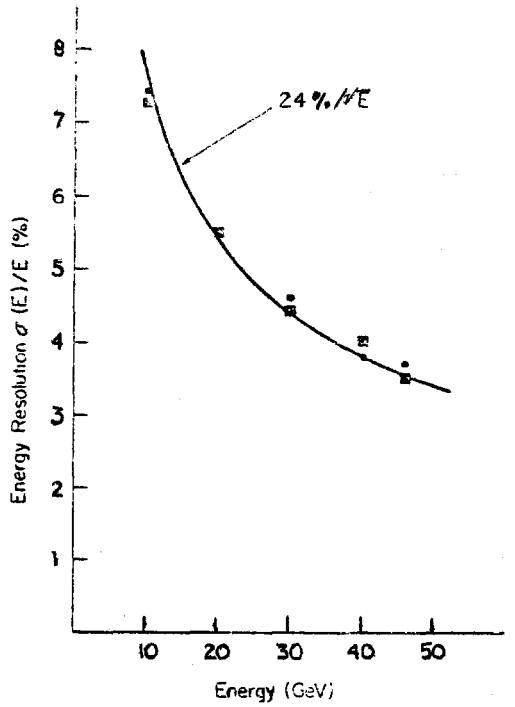

Fig. 7. Wire energy resolution. Resolution from the sum of all three sections is indicated by ●, resolution from section 1 and 2 sum only is indicated by ■.

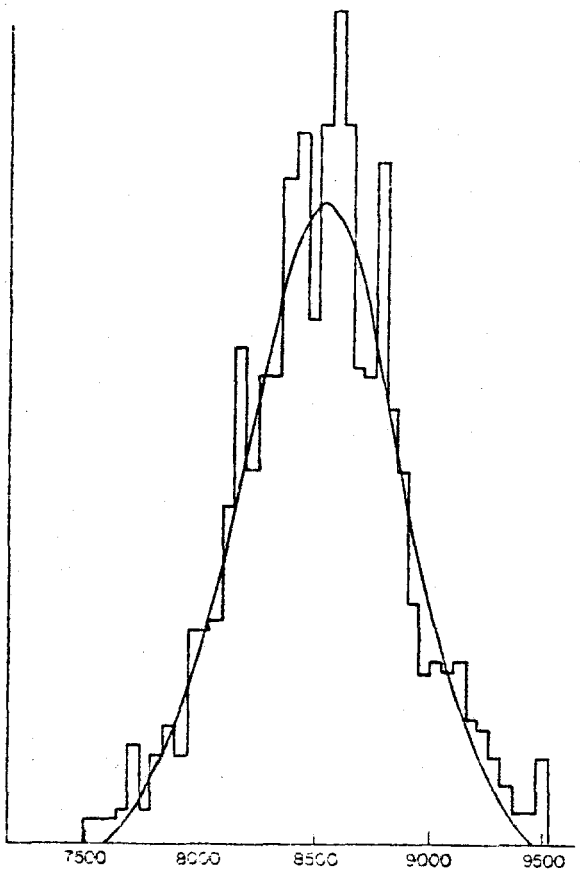

Fig. 8. 40 GeV electron wire signal with least squares fitted Gaussian.

Position resolution was measured at several energies for both the first and second sections. The positions of incident electrons were calculated using both the first and second moment of the lateral energy distribution. The difference between the calculated position and the particle position as measured by a drift chamber was used for position resolution determination. As seen in Fig. 9, the first section gave better resolution than the second. Also, the second moment calculation, which weights the large signal channels more than the low signal channels, gave significantly more accurate position information than the first moment calculation. First section, second moment position resolution was 1.24 mm at 10 GeV and 0.84 mm at 46 GeV.

There was no significant difference in the position resolution of the wires versus the strips for either section or calculation method.

Studies were done to determine the effect on the total calorimeter signal and energy resolution as data were incrementally discarded from one side or both sides of the shower.

Shower position was calculated using the lateral energy distribution. The detector was made symmetric around the shower by determining the distance to the closest edge and discarding enough channels from the other edge to make both distances equal in each section. Then, since the first section had a smaller instrumented area than the others, some of the remaining channels from the second and third sections were discarded so as to make the size of the instrumented areas the same in all sections. The resulting detector measured 14 channels by 14 channels, or 16.8 x 16.8 cm^2. This configuration represents the point of zero channels cut in Figs. 10, 11, and 12.

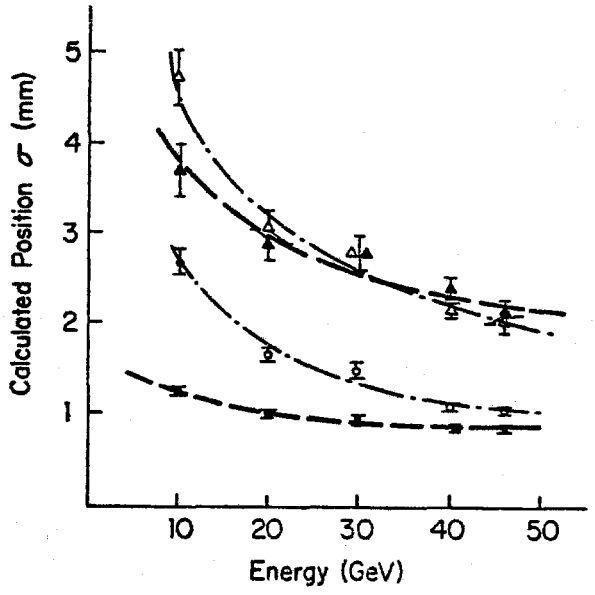

Fig. 9. Position resolution for electrons as a function of incident energy. Position was calculated using either the first or second moment of the lateral energy distribution in both sections 1 and 2.

△ is first moment in section 2

▲ is second moment in section 2

○ is first moment in section 1

● is second moment in section 1

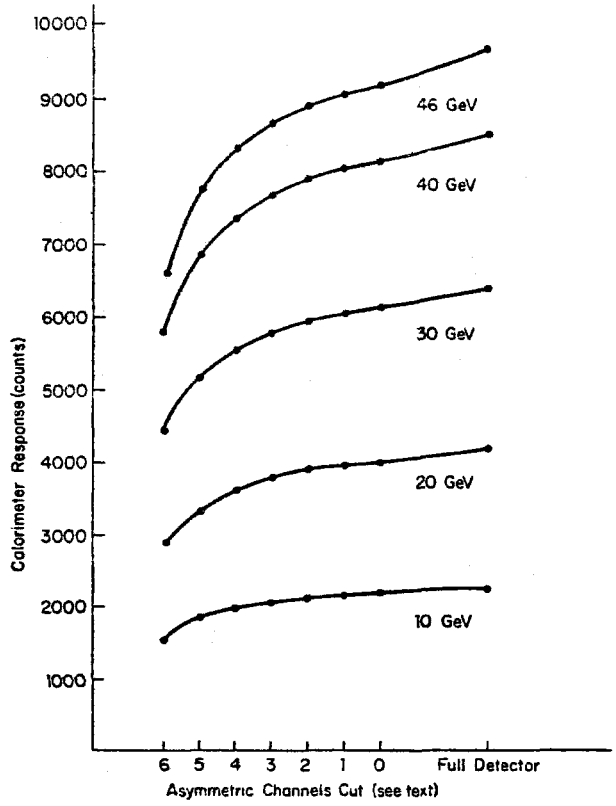

Fig. 10. Calorimeter wire signal versus number of channels cut from one side of the shower only. See text for discussion.

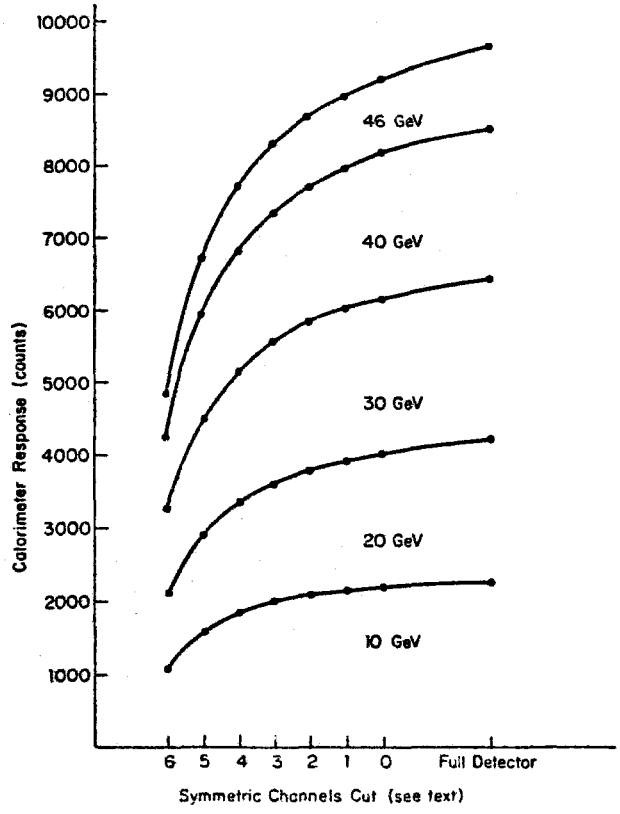

Fig. 11. Calorimeter wire signal versus number of channels cut symmetrically from both shower edges. See text for discussion.

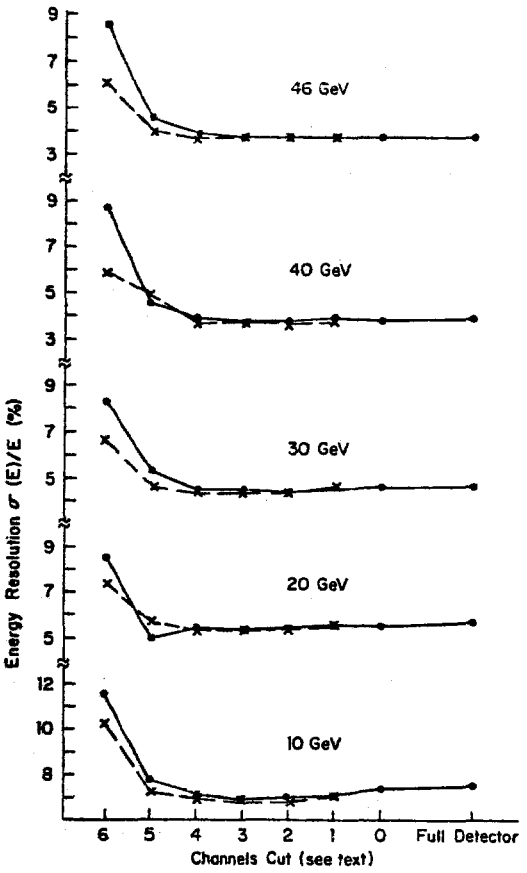

Fig. 12. Energy resolution for wires as a function of the number of channels cut from one edge of the shower (●), or symmetrically from both edges (x). See text for discussion.

Fig. 10 shows how the total wire signal varies when one starts with the above described configuration and removes channels from one side of the detector only. Comparison with the full detector response shows that from 3.4% at 10 GeV to 4.7% at 46 GeV of the signal was lost when the detector was reduced to its initial configuration. The points corresponding to six channels cut describe a detector eight channels wide (9.6 cm), with the shower core between the seventh and eighth cells.

Fig. 11 shows the wire signal as a function of symmetric cuts on both detector edges. The final points with six channels symmetrically cut describe a detector two channels wide with the electron shower core between those two channels.

Fig. 12 shows how the energy resolution changes as a function of both symmetric and asymmetric cuts. Interestingly, the resolution shows some improvement, particularly at lower energies, as one discards the extreme shower edges. Also note that the resolution resulting from two channels alone (six channels cut symmetrically) is considerably better than the resolution resulting from an asymmetric cut of six channels, where one wing is included.

Hadron rejection was measured at 40 GeV only. A lead brick was inserted far upstream of the detector to attenuate the electron fraction prior to trigger formation. Fig. 13 shows the pion peak with a superimposed curve showing the position of the 40 GeV electron peak.

Applying a total signal cut 7.1 GeV wide centered on the 40 GeV electron peak discarded about 2% of the electrons. The resulting pion rejection factor was 8.4×10^{-3}. An additional cut was made on the section 1 signal. Discarding 10% of the electrons, the two cuts together gave a rejection factor of 4×10^{-4}. Fig. 14 shows the application of those cuts to the pion signal.

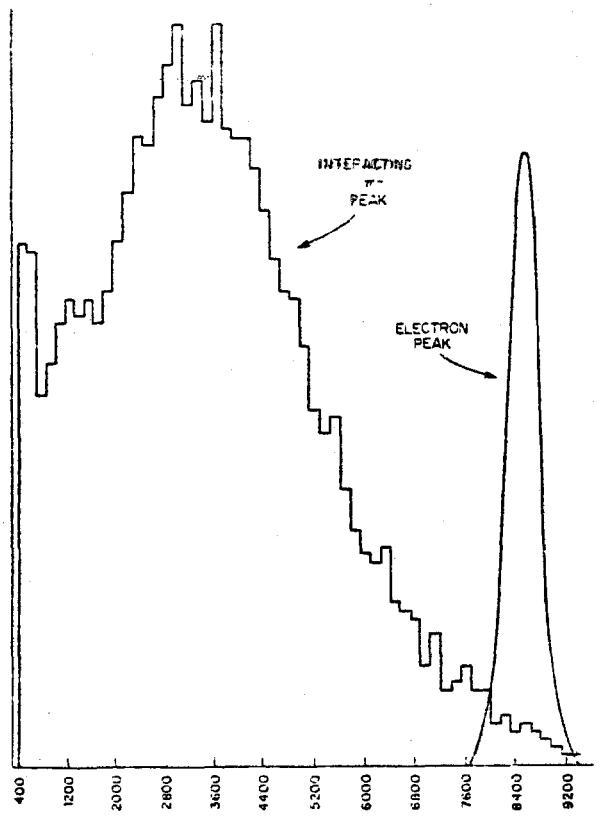

Fig. 13. 40 GeV pion peak showing position of 40 GeV electron peak on same scale. The minimum ionizing peak is not shown.

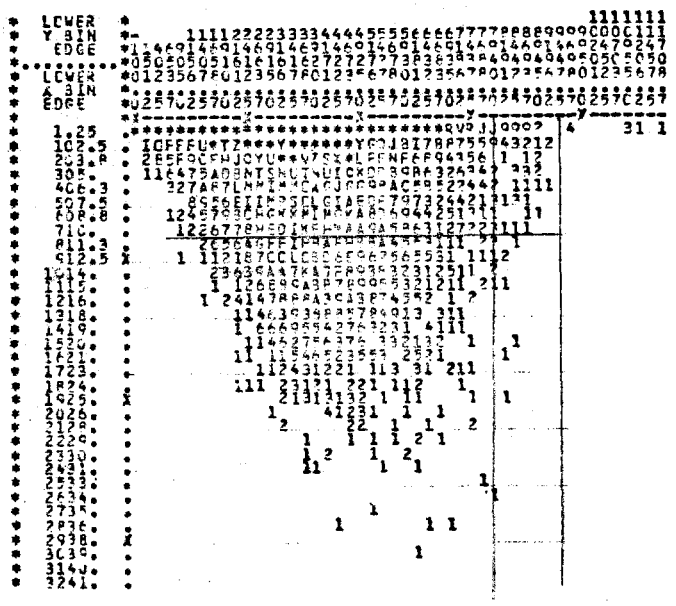

Fig. 14. Correlation plot of total calorimeter signal (horizontal axis) against first section signal (vertical axis) for 40 GeV pions. Lines show the position of the cuts used to determine the pion rejection factor.

Acknowledgments

We would like to thank Dr. M. Mishina, Dr. J. Sauer, W. Coleman, M. Davis, M. Hrycyk, and E. Mabeus for their help in conducting these tests.

References

1. R. L. Anderson, W. W. Ash, D. B. Gustafson, K. Rich, D. M. Ritson, J. R. Johnson, R. Freeport, and D. E. Wiser, IEEE NS-25 (1978) 340.

2. P. Skubic, F. Sannes, D. Potter, J. J. Mueller, R. Imlay, G. K. Chang, and D. Bechis, contributed to this conference.

3. T. F. Droege, M. C. Hibbard, C. A. Nelson, Jr., P. A. Thompson, Y. Makdisi, R. Lipton, IEEE NS-27 (1980) 64.

4. J. F. Bartlett, J. R. Biel, D. B. Curtis, R. J. Dosen, T. D. Lagerlund, D. J. Ritchie, and L. M. Taff, IEEE NS-26 (1979) 4427.

*Operated by Universities Research Association under Contract with the United States Department of Energy.